An LPV Control Approach for a Fuel Cell Power Generator Air Supply System

David Hernández-Torres, Olivier Sename, Delphine Riu

An LPV Control Approach for a Fuel Cell Power Generator Air Supply System

David Hernández-Torres [1], Olivier Sename[2] and Delphine Riu[1],

***Abstract*— In this paper, the control of the air supply system of a fuel cell power generator is addressed. The management of the air dynamic entering the fuel cell is assured by the control of the air flow of a compressor. The air supply sub-system is controlled to keep a desired oxygen excess ratio, this allows to improve the fuel cell performance. Linear Matrix Inequalities (LMI) tools are extensively used in this paper as a solution to the multivariable robust control problem. Robust multivariable $\mathcal{H}_\infty$ controllers are considered. A special interest is also given to reduced order controllers, specifically simple PI structures with desired $\mathcal{H}_\infty$ performances. The models used for control implementation were identified from measures on a real test-bench set-up. Two control strategies are proposed, first a speed controller for the air compressor is designed; then the problem of a robust control of the system subject to some model uncertainties is solved using the Linear Parameter Varying (LPV) approach. The validation of the closed-loop control strategies is achieved using time-domain simulation analysis and the gain scheduled approach.**

I. Introduction

Fuel cells (FC) are very attractive electro-chemical energy conversion devices because they are a proper emission-free technology. It is expected that FC will play a very important role in future Distributed Generation (DG) applications [1]. FC's operating as DG can be connected to the utility grid or can be operated as stand-alone power supply systems in a remote areas [2]. There is an increasing number of commercially available FC as backup units for isolated and secure communication and telecoms applications [3].

Despite a working principle that was discovered more than 150 years ago, there has been an important development in FC technology in the last decades. Beginning with its first commercial use during NASA's Gemini project in 1965 to its actual state of development, which has achieved a very important maturity. Certainly this development has been boosted by the global warming threat and the need of an alternative to the fossil-hydrocarbon based energy. Moreover in recent years, the energy prices and the cleanliness of actual energy sources, the depletion of oil wells, the imminent reach of the peak-oil point, and several other conditions have accelerated this process, not only with FC but with other types of renewable energy.

When referring to a FC system, all the auxiliary systems, needed for operation, are included. This makes the complete system a rather complex structure to control. Some robust control strategies, including the use of reduced order controllers (PI or reduced order $\mathcal{H}_\infty$), have already been proposed by the authors in previous works [4], [5]. However these works were devoted to the power management of the electrical sub-system of the FC. On the other hand this paper focuses on the thermo-dynamical sub-system management, and more precisely, on the air supply system. A complete summary of compressor types and technologies is presented in [6]. For the compressor-motor system modeling, we have focused our attention on control-oriented models. We have considered the non-linear model proposed in [7], which is a reduced order version of the non-linear model proposed in the book [8]. Several elegant results on FC and compressor-motor group control have been proposed in the literature to optimize the net power and reduce the energy consumption of the whole group. Optimization techniques for FC generators including compressor-motor group using particle swarm optimization and extremum seeking approach have been presented in [9] and [10] respectively. Other approaches for the FC air supply control system may include non-linear control, as in [11] where passivity control is used on the reduced order non-linear model proposed by [7]. An interesting analysis on FC performance at different loading conditions and a valuable contribution on a strategy to compute the compressor speed reference signal may be found in [12].

The control objectives considered are both the tracking problem and the disturbance regulation. The optimization of reference signals using dedicated algorithm is not addressed in this paper. However a rich literature can be found on this subject, control strategies can be based on imposed reference signals related to the FC dynamic, using for example a Maximum Power Point Tracker (MPPT) algorithm or a tracking on the FC efficiency curve. See [2], [13], [14], [15] or even [16] for several examples on primary level control methodologies.

This paper is divided in two main parts. First the identified model for the air supply system is introduced, then the affine LPV models of these systems are developed and the obtained control results are presented. The control methodology and the basis of the LPV approach considered are presented in the appendix section.

II. System modeling and identification

The reduced 4^{th} order control-oriented model described here was developed in [7], as a manipulation of the complete 9^{th} order model presented in [8]. In order to obtain control-oriented models, this system considers that the fuel flow

[1] D. Hernández-Torres and D. Riu are with Grenoble Electrical Engineering Laboratory, 38400 Saint-Martin-D'Hères, France Email: delphine.riu@g2elab.grenoble-inp.fr

[2] O. Sename is with GIPSA-Lab, Department of Control Systems, 38400 Saint-Martin-D'Hères, France Email: olivier.sename@gipsa-lab.grenoble-inp.fr

control, the air humidification and the stack temperature controls are perfect. A model reduction is then possible.

From the dynamical equations in the FC cathode, the supply manifold, and the air compressor, the following set of equations may be obtained:

$$\begin{aligned}
\frac{dp_{O_2}}{dt} &= \frac{\mathcal{R}T_{st}}{\mathcal{M}_{O_2}V_{ca}}(W_{O_2,ca,in} - W_{O_2,ca,out} - W_{O_2,reacted}) \\
\frac{dp_{N_2}}{dt} &= \frac{\mathcal{R}T_{st}}{\mathcal{M}_{N_2}V_{ca}}(W_{N_2,ca,in} - W_{N_2,ca,out}) \\
\frac{dp_{sm}}{dt} &= \frac{\mathcal{R}_a T_{cp}}{V_{sm}}(W_{cp} - W_{ca,in}) \\
\frac{d\omega_{cp}}{dt} &= \frac{1}{J_{cp}}(\tau_{cm} - \tau_{cp})
\end{aligned} \tag{1}$$

with p_{O_2} and p_{N_2} the oxygen and nitrogen partial pressures in the FC, W denotes the several flows, T_{st} is the stack temperature, $\mathcal{R}$ is the universal gas constant, $\mathcal{M}$ is the molar mass, V_{ca} is the cathode volume, J_{cp} is the compressor inertia constant and τ symbolizes the motor or compressor torques. Subscripts ca, sm and cp designates the FC cathode, the supply manifold and the air compressor respectively.

This model is highly non-linear, due to the non-linearities involved in the air compressor model. See [8] or [7] for more details on this model. Now, the system equations are resumed using exactly the same system notation as in [11], which is a more simplistic presentation designed for control purposes. The resumed model equations presented here correspond to the further model reduction proposed in the interesting work [11]. This further reduction has an important physical meaning for the system, since a new dynamic variable, the cathode air pressure $\chi = p_{air,ca}$ is defined.

The system (1) is given in the form:

$$\dot{x} = f(x) + g_u u + g_\xi \xi \tag{2}$$

where the state vector is given by:

$$x = \begin{bmatrix} x_1 & x_2 & x_3 & x_4 \end{bmatrix}^T = \begin{bmatrix} p_{O_2} & p_{N_2} & \omega_{cp} & p_{sm} \end{bmatrix}^T \tag{3}$$

The new change of coordinates is defined by:

$$\chi = x_1 + x_2 + c_2 \tag{4}$$

Then the following third-order model is obtained:

$$\begin{aligned}
\dot{\chi} &= -\mu_1\chi + \mu_2 x_4 + \mu_3 - \mu_4\xi \\
\dot{x}_3 &= -c_9 x_3 - \frac{c_{10}}{x_3}\left[\left(\frac{x_4}{c_{11}}\right)^{c_{12}} - 1\right] h_3(x_3, x_4) + c_{13}u \\
\dot{x}_4 &= c_{14}\left[1 + c_{15}\left[\left(\frac{x_4}{c_{11}}\right)^{c_{12}} - 1\right]\right][h_3(x_3, x_4) - \cdots \\
&\quad c_{16}\left(-\chi + x_4\right)]
\end{aligned} \tag{5}$$

with:

$$\mu_1 = c_1 + c_8 + \frac{c_3 c_{20}}{\kappa},\ \mu_2 = c_1 + c_8,\ \mu_3 = \frac{c_2 c_3 c_{20}}{\kappa},\ \mu_4 = c_7$$

The system constants are well defined in [11]. An important characteristic of this system is that it can be separated into several sub-system. This is presented in Figure 1. The outputs of the system are $x_4 = p_{sm}$ the supply manifold pressure, $h_1(x_1, x_2) = V_{st}$ the FC stack voltage and $h_3(x_3, x_4) = W_{cp}$ the compressor air flow. The inputs are ξ, the fuel cell current, and u, the supply voltage of the compressor motor. The system Σ_χ is given by the first equation in system (5). Subsequently systems Σ_{x_3} and Σ_{x_4} are respectively given by the second and third equations in (5).

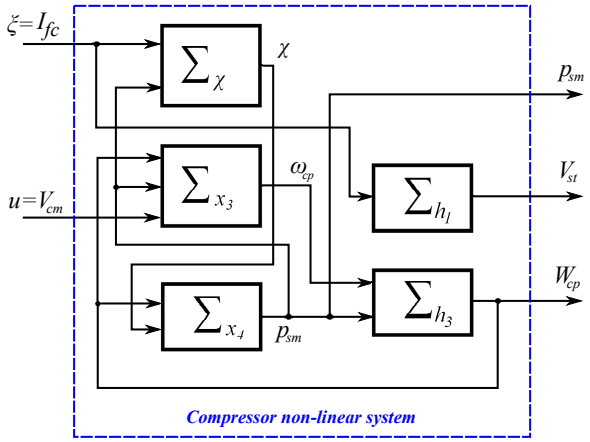

Fig. 1. Non-linear FCS model.

The several models parameters were identified separately for each sub-system. The complete identification methodology, including the presentation of the test-bench set-ups used to obtain the real system measures are presented in [17]. Models parameters identification results are given in Table I.

TABLE I

MODEL PARAMETERS

Dynamic eq. in χ	Value	Dynamic eq. in x_3	Value
μ_1	-399.3	c_9	2300
μ_2	391.2	c_{10}	774.7
μ_3	350	c_{13}	1069.5
μ_4	-7718.8		

While the model (5) is reduced, it is not fitting well the benchmark experimental data (see [17]). In particular, some internal loops in the benchmark lead to some additional dynamics that have to be taken into account.

To cope with this problem, a linear state-space model for the cathode pressure dynamic was identified. The obtained model for the system dynamic of x_4 is given in the form:

$$\Sigma_{x_4} \begin{cases} \dot{x} &= Ax + Bu \\ y &= Cx + Du \end{cases}$$

with:

$$A = \begin{bmatrix} -0.029 & -7.451 \\ 7.451 & -21.51 \end{bmatrix}, C = \begin{bmatrix} -2231 & -5.512 \times 10^4 \end{bmatrix}$$
$$B = \begin{bmatrix} 2231 & -5.013 \times 10^{-6} \\ -5.512 \times 10^4 & 1.156 \times 10^{-5} \end{bmatrix}$$
$$D = \begin{bmatrix} 3.964 \times 10^7 & -0.01884 \end{bmatrix}$$

where input vector is given by $u = \begin{bmatrix} h_3(x_3, x_4) & \chi \end{bmatrix}^T$ and the system output is $y = x_4$.

Linear state-space systems were also identified to model the dynamic of the stack voltage $h_1(x_1, x_2)$ and the air compressor flow $h_3(x_3, x_4)$ (see [17] for the complete identification results).

III. Affine Quasi-LPV models

From the identified models described before, the goal now is to find affine quasi-LPV models for robust control computation. Given the non-linearities and avoiding the possibility of a high number of varying parameters, three propositions are presented. In these propositions the systems may be separated in the cascade form (cf to the system model diagram presented in Figure 1). In the first proposition, an LPV affine system representation considering all model state-space variables (χ, x_3, x_4) is presented. The second and third propositions are a reduction of the first method, then considering subsequently affine LPV models of sub-systems (χ, x_3) and (x_3, x_4) respectively.

A. First method: Full reduced-order LPV system

From the original system we define a first varying parameter given by:

$$\rho_1 = -\frac{c_{10}}{x_3 x_4}\left[\left(\frac{x_4}{c_{11}}\right)^{c_{12}} - 1\right] h_3(x_3, x_4) \tag{6}$$

With this, the equation in x_3 becomes:

$$\dot{x}_3 = -c_9 x_3 + \rho_1 x_4 + c_1 3u \tag{7}$$

To parametrize the equation in x_4 we define:

$$\rho_2 = \frac{c_{14}}{x_3}\left[1 + c_{15}\left[\left(\frac{x_4}{c_{11}}\right)^{c_{12}} - 1\right]\right] h_3(x_3, x_4) \tag{8}$$
$$\rho_3 = c_{14} c_{16}\left[1 + c_{15}\left[\left(\frac{x_4}{c_{11}}\right)^{c_{12}} - 1\right]\right] \tag{9}$$

Some conservatism may then appear noting moreover that ρ_2 and ρ_3 are linked by:

$$\rho_2 = \rho_3 \frac{h_3(x_3, x_4)}{c_{16} x_3} \tag{10}$$

A fourth parameter may be defined as:

$$\rho_4 = \mu_2 + \frac{\mu_3}{x_4} \tag{11}$$

With this the complete system becomes:

$$\begin{cases} \dot{\chi} &= -\mu_1 \chi + \rho_4 x_4 - \mu_4 \xi \\ \dot{x}_3 &= -c_9 x_3 + \rho_1 x_4 + c_{13} u \\ \dot{x}_4 &= \rho_2 x_3 - \rho_3 x_4 + \rho_3 \chi \end{cases} \tag{12}$$

The block diagram in Figure 1 can still be considered to obtain the complete model connections between the sub-systems.

B. Second method: An LPV (χ, x_3) model

For this approach, a reduction of the full reduced-order LPV system, the following varying parameters are considered:

$$\rho_1 = \mu_2 + \frac{\mu_3}{x_4} \tag{13}$$
$$\rho_2 = -\frac{c_{10}}{x_3 x_4}\left[\left(\frac{x_4}{c_{11}}\right)^{c_{12}} - 1\right] h_3(x_3, x_4) \tag{14}$$

The obtained LPV sub-system is given by:

$$\begin{cases} \dot{\chi} &= -\mu_1 \chi + \rho_1 x_4 - \mu_4 \xi \\ \dot{x}_3 &= -c_9 x_3 + \rho_2 x_4 + c_{13} u \end{cases} \tag{15}$$

The LPV system block diagram of the system considering the second method is given in Figure 2.

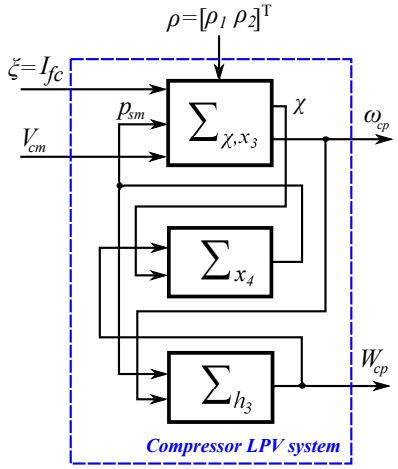

Fig. 2. Compressor LPV system block diagram for an LPV (χ, x_3) model (second method)

C. Third method: Towards an LPV (x_3, x_4) model

In this third method, we keep the notation presented for the full reduced order LPV system (first method), but we decouple the equation of χ from the system. The reduced LPV sub-system obtained is then given by:

$$\begin{cases} \dot{x}_3 &= -c_9 x_3 + \rho_1 x_4 + c_{13} u \\ \dot{x}_4 &= \rho_2 x_3 - \rho_3 x_4 + \rho_3 \chi \end{cases} \tag{16}$$

As an advantage using this approach the remaining sub-system in χ is linear and easy to control.

The non-linear model equations are used to obtain time-domain simulations. From these simulations, it has been noted that the variation range of ρ_3 is negligible. The value of ρ_3 is constant at 7.342×10^{-5} for a variation range of the FC current from 22 to 39A and of the compressor-motor control voltage from 237 to 300V. The LPV model is finally reduced to two varying parameters. Using non-linear simulations and the identified model parameters, the varying parameters range is given by:

$$\rho_1 \in [2.577 \times 10^{-5}, 2.388 \times 10^{-4}]$$
$$\rho_2 \in [4200, 38068]$$

The compressor LPV system block diagram considering the third method is given in Figure 3.

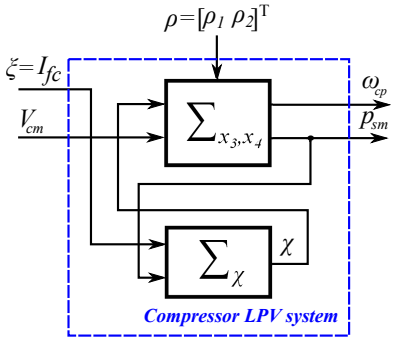

Fig. 3. Compressor LPV system block diagram for an LPV (x_3, x_4) model (third method).

IV. LPV CONTROL AND RESULTS

In this section the results obtained for LPV controller implementation are presented. Two main problems are solved. The first represent the control problem of the non-linear compressor system using the quasi-affine LPV model (given in the third method). In the second problem, some model uncertainties are considered, to solve this problem the quasi-affine LPV model presented in the second method is used.

A. Solution to the control of the non-linear compressor model

For convenience, we will keep the proposed affine model for sub-system (x_3, x_4). The proposed control configuration using gain scheduling and including the performance weighting functions, is presented in Figure 4.

The cut-off frequency ω_B is fixed for a sufficient fast speed response. The weighting function is given by:

$$W_{perf} = \frac{500s + 2000}{s + 0.002}$$

A full order $\mathcal{H}_\infty$ polytopic controller is computed with a conditioning number $\gamma = 1.3478$. The singular values plot of the sensitivity function at each corner of the polytope is given in Figure 5.

It shows that the closed-loop system achieves good disturbance rejection at each polytopic vertex, however the

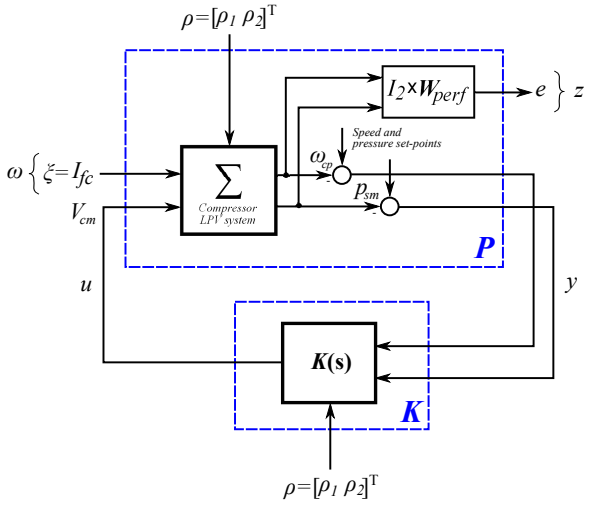

Fig. 4. Control configuration in the P-K form for the LPV system.

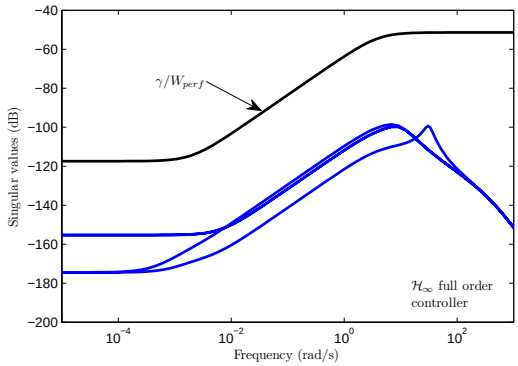

Fig. 5. Singular values plot of the sensitivity function for $\mathcal{H}_\infty$ polytopic controller.

validation inside the polytopic set is provided to verify the control performances. For this we use the gain scheduling approach. The gain scheduled controller simulation was obtained using SIMULINK and the given functions for polytopic set definition: `pvec` and `polydec`. The system response to a FC load step and the system response to the tracking problem of the speed reference signal are presented in Figures 6 and 7 respectively. These results demonstrate the effectiveness of the speed control strategy proposed, robust to parameter variations in the model. In the following section a similar problem is treated for the solution of the control problem of a system subject to model uncertainties. The parameter variation trajectory used for time-domain simulations is presented in Figure 8.

B. Model uncertainties problem solution

Following a similar approach, the problem of a model subject to uncertainties is now solved using LPV control.

The proposed control configuration using gain scheduling and including the performance weighting functions, is identical to the previous case, in contrast the compressor LPV model is given by the sub-system (χ, x_3) (cf to the second proposed method). From this system, parameters c_9

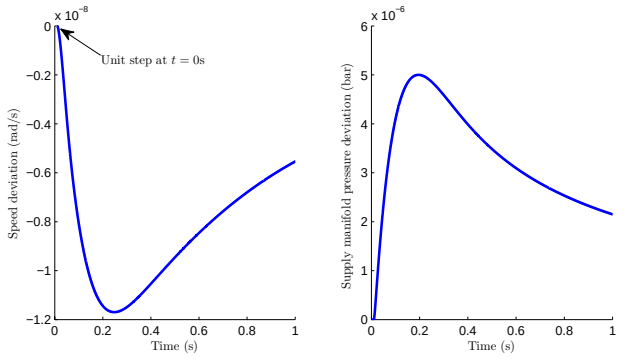

Fig. 6. System response to a load step using gain scheduling approach.

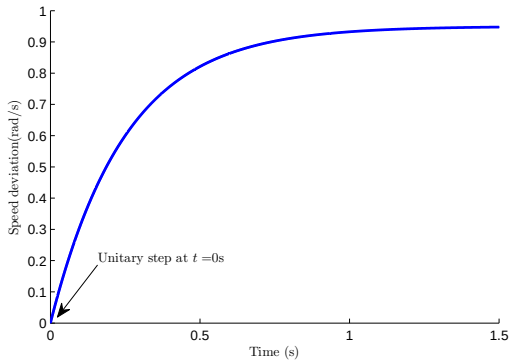

Fig. 7. System response to a speed reference step using gain scheduling approach.

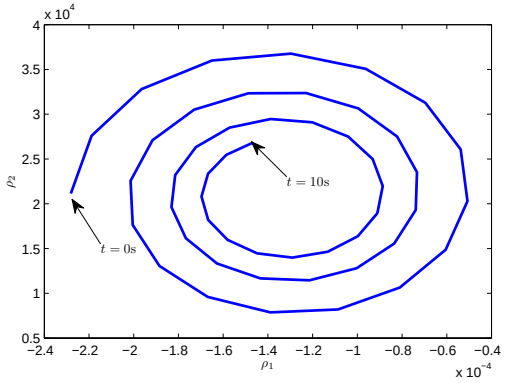

Fig. 8. Varying parameter trajectory.

and c_{13} of the 3^{rd} order non-linear system are assumed to be uncertain. These parameters are directly dependent on the compressor-motor inertia constant J_{cp}, which may assumed to be variable or with uncertainty on its identified value.

From simulations of the non-linear model, the bounds of the varying parameters have been estimated as:

$$\rho_1 = c_9 \in [930.26, 2300]$$
$$\rho_2 = c_{13} \in [1069.5, 3531.7]$$

From these values, the model is linearized for given steady-state values of $x_{3_e} = 110$rad/s and $x_{4_e} = 1.512$bar, to obtain a state-space representation in the form $\dot{x} = Ax + Bu$, with state matrices:

$$A = \begin{bmatrix} -\mu_1 & 0 \\ 0 & -\rho_1 \end{bmatrix} \text{ and } B = \begin{bmatrix} k_2 & -\mu_4 & 0 \\ k_1 & 0 & \rho_2 \end{bmatrix} \tag{17}$$

with:

$$k_1 = -\frac{c_{10}}{x_{3_e} x_{4_e}} \left[\left(\frac{x_{4_e}}{c_{11}} \right)^{c_{12}} - 1 \right] h_3(x_{3_e}, x_{4_e}) \tag{18}$$

$$k_2 = \mu_2 + \frac{\mu_3}{x_{4_e}} \tag{19}$$

where $x = \begin{bmatrix} \chi & x_3 \end{bmatrix}^T$ and $u = \begin{bmatrix} x_4 & \xi & V_{cm} \end{bmatrix}^T$.

Both a full order $\mathcal{H}_\infty$ polytopic controller and a PI LPV controller are computed following the methodology described in the appendix. The weighting functions for the $\mathcal{H}_\infty$ and PI controllers are respectively given by:

$$W_{perf_{\mathcal{H}_\infty}} = \frac{500s + 20000}{s + 0.02}$$
$$W_{perf_{PI}} = \frac{50s + 20000}{s + 20}$$

The performance level for each controller are $\gamma_{\mathcal{H}_\infty} = 210.96$ and $\gamma_{PI} = 5.72$. The closed-loop systems are stable for each corner of the polytopic representation, however the PI LPV controller is not gain scheduled, i.e. the obtained controller is not parameter-dependent, because given the methodology described in [4], [5], the matrix D_{22} of the state-space model is parameter independent. As before, the singular values plot of the sensitivity function for $\mathcal{H}_\infty$ polytopic and the PI LPV controllers are shown in Figure 9. More robustness is obtained with the $\mathcal{H}_\infty$ polytopic control.

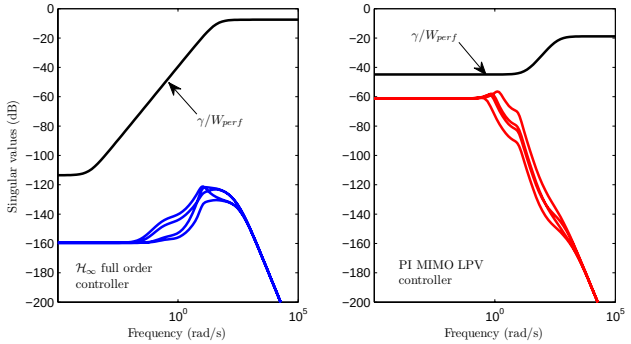

Fig. 9. Singular values plot of the sensitivity function for $\mathcal{H}_\infty$ polytopic and PI LPV controllers.

The control procedure is validated from time-domain simulation results using gain scheduled systems. The system response to a FC load step is presented in Figure 10. The defined parameter variation trajectory used for gain scheduled simulation is presented in Figure 11. The closed-loop simulation results show a good disturbance rejection for the $\mathcal{H}_\infty$ polytopic controller, however an undesired overshoot appears in the speed reference tracking response.

Despite this, the system remains stable for the uncertainties level defined. Disturbance rejection and reference tracking performances are not entirely meet by the PI LPV controller.

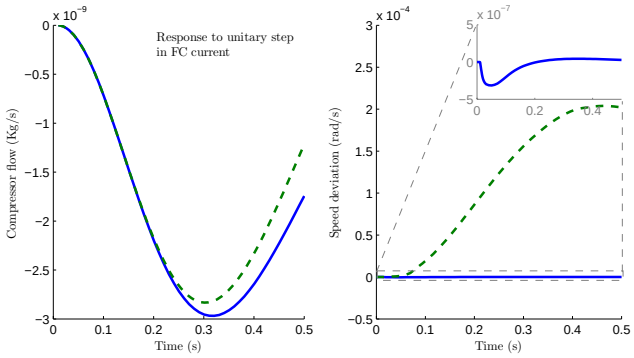

Fig. 10. System response to a load step using gain scheduling approach ($\mathcal{H}_\infty$ polytopic controller in continuous line and PI LPV controller in dashed line).

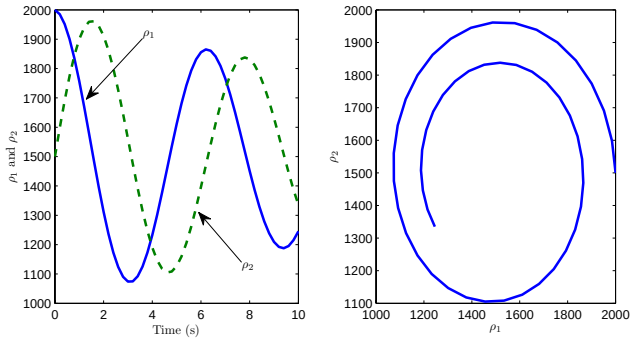

Fig. 11. Varying parameter trajectory.

V. Conclusion

An interesting multivariable robust control methodology for LPV systems is proposed in this paper. In general good results were obtained achieving the goal of a disturbance rejection or tracking control problem. In some specific cases, the disturbance effective rejection mitigates the harmful effects of large load transients on the FC, preserving its life span. The results obtained emphasize the interest of the LPV methodology which needs to be further studied. An important perspective for future works may be design an LPV control approach for a more wide operating range, and then include the influence of temperature and cell humidification in the FC operating point. Comparing the proposed strategies with classical control approaches should be also envisaged.

References

[1] C. Wang and M. H. Nehrir, "Load Transient Mitigation for Stand-Alone Fuel Cell Generation Systems," *IEEE Trans. on En. Conv.*, vol. 22, pp. 864–872, Dec. 2007.

[2] Y. S. Han, S. Li, X. Park, S. Jeong, H. Jung, and B. Jung, "A power control scheme to improve the performance of a fuel cell hybrid power source for residential application," in *Power Electronics Specialists Conference, 2007. PESC 2007. IEEE*, June 2007, pp. 1261 – 1266.

[3] H. Tao, J. L. Duarte, and M. A. M. Hendrix, "Line-interactive ups using fuel cell as the primary source," *IEEE Trans. Ind. Electron.*, vol. 55, no. 8, pp. 3005–3011, Aug 2008.

[4] D. Hernandez-Torres, D. Riu, O. Sename, and F. Druart, "Robust optimal control strategies for a hybrid fuel cell power management system," in *36th Annual Conference on IEEE Industrial Electronics Society IECON*, Nov. 7–10 2010, pp. 698–703.

[5] ——, "On the Robust Control of DC-DC Converters: Application to a Hybrid Power Generation System," in *4th IFAC Symposium on system, structure and control SSSC*, Sep. 15–17 2010.

[6] B. Blunier, "Modélisation de moto-compresseurs en vue de la gestion de l'air dans les systèmes piles à combustible, simulation et validation expérimentale (in French)," Ph.D. dissertation, Université de Technologie de Belfot-Montbéliard,, Belfort, 2007.

[7] K. W. Suh, "Modeling, Analysis and Control of Fuel Cell Hybrid Power Systems," Ph.D. dissertation, Department of Mechanical Engineering, The University of Michigan, 2006.

[8] J. T. Pukrushpan, A. G. Stefanopoulou, and H. Peng, *Control of Fuel Cell Power Systems. Principles, Modeling, Analysis and Feedback Design*, A. in Industrial Control, Ed. Springer, 2004.

[9] M. Tekin, D. Hissel, M.-C. Pera, and J.-M. Kauffmann, "Energy consumption reduction of a PEM fuel cell motor-compressor group thanks to efficient control laws," *Journal of Power Sources*, vol. 156, pp. 57–63, July 2006.

[10] Y. A. Chang and S. J. Moura, "Air Flow Control in Fuel Cell Systems: An Extremum Seeking Approach," in *IEEE American Control Conference*, St. Louis, MO, USA, June 2009, pp. 1052–1059.

[11] R. Talj, R. Ortega, and M. Hilairet, "A controller tuning methodology for the air supply system of a PEM fuel-cell system with guaranteed stability properties," *International Journal of Control*, vol. 82, no. 9, pp. 1706–1719, Sep. 2009.

[12] D. Thirumalai and R. White, "Steady-state operation of a compressor for a proton exchange membrane fuel cell system," *Journal of Applied Electrochemistry*, vol. 30, pp. 551–559, 2000.

[13] P. Thounthong, S. Raël, and B. Davat, "Energy management of fuel cell/battery/supercapacitor hybrid power source for vehicle applications," *Journal of Power Sources*, no. 193, pp. 376 – 385, 2009.

[14] P. Thounthong and S. Rael, "The benefits of hybridization," *Industrial Electronics Magazine, IEEE*, vol. 3, no. 3, pp. 25–37, Sep. 2009.

[15] K.-W. Suh and A. G. Stefanopoulou, "Coordination of converter and fuel cell controllers," *International Journal of Energy Research*, vol. 29, no. 12, pp. 1167–1189, 2005.

[16] I. Valero, S. Bacha, and E. Rulliere, "Comparison of energy management controls for fuel cell applications," *Journal of Power Sources*, vol. 156, no. 1, pp. 50–56, 2006, selected papers from the 2nd France-Deutschland Fuel Cell Conference.

[17] D. Hernandez-Torres, "Commande robuste de générateurs électrochimiques hybrides," Ph.D. dissertation, Université de Grenoble, Grenoble, France, 2011.